



저작자표시-비영리-변경금지 2.0 대한민국

이용자는 아래의 조건을 따르는 경우에 한하여 자유롭게

- 이 저작물을 복제, 배포, 전송, 전시, 공연 및 방송할 수 있습니다.

다음과 같은 조건을 따라야 합니다:



저작자표시. 귀하는 원저작자를 표시하여야 합니다.



비영리. 귀하는 이 저작물을 영리 목적으로 이용할 수 없습니다.



변경금지. 귀하는 이 저작물을 개작, 변형 또는 가공할 수 없습니다.

- 귀하는, 이 저작물의 재이용이나 배포의 경우, 이 저작물에 적용된 이용허락조건을 명확하게 나타내어야 합니다.
- 저작권자로부터 별도의 허가를 받으면 이러한 조건들은 적용되지 않습니다.

저작권법에 따른 이용자의 권리는 위의 내용에 의하여 영향을 받지 않습니다.

이것은 [이용허락규약\(Legal Code\)](#)을 이해하기 쉽게 요약한 것입니다.

[Disclaimer](#)

이학박사 학위논문

지방 유래 중간엽 줄기세포 노화 과정에서
SPHK1 의 역할 규명

The role of SPHK1 on the development of cellular senescence
in human adipose-derived stromal cells

울산대학교 대학원
의 학 과
김 민 경

지방 유래 중간엽 줄기세포 노화 과정에서
SPHK1의 역할 규명

지도교수 김승후

이 논문을 이학박사 학위 논문으로 제출함

2021년 02월

울산대학교 대학원

의학과

김민경

김민경의 이학박사학위 논문을 인준함

심사위원 장 은 주 인

심사위원 최 경 철 인

심사위원 최 순 철 인

심사위원 김 미 라 인

심사위원 김 승 후 인

울산대학교 대학원

2021년 02월

ABSTRACT

We have identified a mechanism to diminish the proliferation capacity of cells during cell expansion by using human adipose-derived stromal cells (hAD-SCs) as a model of replicative senescence. hAD-SCs of high passage numbers exhibited a reduced proliferation capacity with accelerated cellular senescence. The levels of key bioactive sphingolipids were significantly increased in these senescent hAD-SCs. Notably, transcription of sphingosine kinase 1 (SPHK1) was down-regulated in hAD-SCs at high passage numbers. SPHK1 knockdown as well as inhibition of its enzymatic activity impeded proliferation of hAD-SCs, with concomitant induction of cellular senescence and accumulation of sphingolipids as in high passage cells. SPHK1 knockdown-accelerated cellular senescence was attenuated by co-treatment of sphingosine-1-phosphate and an inhibitor of ceramide synthesis, fumonisin B1 but not by treatment of either one. Recent research has been uncovered the relationship between SPHK1 and mitochondrial dysfunction. We have shown that mitochondrial ROS, oxygen consumption rate (OCR), and NAD⁺/NADH ratio were powerfully increased, and the metabolic change for gaining energy is biased against glycolysis in knockdown of SPHK1. And we have concluded that the autophagy nucleation step doesn't progress well through ATG5-12 conjugated form was decreased in shSPHK1 cells. Taken together, these results suggest that down-regulated transcription of SPHK1 is a critical inducer of altered

sphingolipid profiles and enhancing dysfunctional mitochondria and replicative senescence during multiple rounds of cell division.

Keywords: Sphingolipid, Sphingosine kinase 1, SPHK1 transcription, Replicative senescence, Mitochondrial dysfunction, Autophagy, Human adipose-derived stromal cell.

CONTENTS

ABSTRACT	i
CONTENTS	iii
LIST OF FIGURES	v
INTRODUCTION	1
MATERIALS AND METHODS	5
Human adipose-derived stromal cells (hAD-SCs)	5
Stable knockdown of SPHK1 and reagents	5
BrdU incorporation	6
Senescence-associated β -galactosidase staining (SA- β -gal staining)	7
Western blotting	7
Quantitative real-time PCR (qRT-PCR)	8
Liquid chromatography-tandem mass spectrometry (LC-MS/MS) for sphingolipids	8
Mitochondrial ROS and Mass	9
Oxygen consumption rate (OCR)	9
NAD assay	10
Glucose uptake / Lactate production	10
Statistical analysis	11

Table 1 Quantitative Real-time PCR (qRT-PCR) primer sequence of sphingolipid metabolic enzymes	12
RESULTS	13
Continuous expansion of hAD-SCs induces cellular senescence	13
Reduced transcription of SPHK1 in senescent hAD-SCs	15
Silencing of SPHK1 leads to cellular senescence	17
Inhibition of enzymatic activity of SPHK1 induces cellular senescence.....	19
Continuous expansion of hAD-SCs leads to accumulation of sphingolipids.....	21
Inhibition of ceramide synthesis does not attenuate senescence accelerated by SPHK1 knockdown.....	23
Supplementation of S1P does not recover senescence enhanced by SPHK1 knockdown·	25
Alteration of sphingolipid profiles causes cellular senescence in SPHK1-depleted cells ·	27
The shRNA-mediate silencing SPHK1 enhances glycolysis and OCR	29
Depletion of SPHK1 induces mitochondrial dysfunction and uncoupling process.....	31
SPHK1 exists in the mitochondria and has an effect on the decrease of autophagy flux·	33
DISCUSSION	36
REFERENCES	42
국문 요약.....	54

List of Figures

Fig. 1. High passage hAD-SCs undergo cellular senescence	14
Fig. 2. Transcription of SPHK1 is reduced in senescent hAD-SCs	16
Fig. 3. Knockdown of SPHK1 promotes cellular senescence.....	18
Fig. 4 Inhibition of enzymatic activity of SPHK1 accelerates cellular senescence.....	20
Fig. 5. Senescent hAD-SCs changes in sphingolipid profile.	22
Fig. 6. Single inhibition of ceramide synthesis does not attenuate senescence accelerated by SPHK1 knockdown.....	24
Fig. 7. Single supplementation of S1P does not recover senescence enhanced by SPHK1 knockdown.....	26
Fig. 8. SPHK1 knockdown-accelerated cellular senescence is attenuated by inhibition of ceramide synthesis and concurrent supplementation of S1P.....	28
Fig. 9. Depletion of SPHK1 enhances glycolysis and OCR	30
Fig. 10. Depletion of SPHK1 induces mitochondrial dysfunction and uncoupling process ..	32
Fig. 11. SPHK1 exists in the mitochondria and has an effect on the decrease of autophagy flux	35

INTRODUCTION

Sphingolipids are essential components of eukaryotic cells and exist in the form of some metabolites including sphingomyelins, ceramides and sphingosine. Besides playing structural roles in cell membrane, they function as bioactive signaling molecules to regulate cell proliferation, differentiation, migration, and apoptosis (1, 2). Sphingolipid metabolic pathways exhibit an intricate network of reactions involving a variety of enzymes. In this pathway, sphingosine is a backbone of all sphingolipids. Sphingomyelins are produced by sphingomyelin synthases using phosphatidylcholine and ceramide (3). Ceramide, a central sphingolipid, is synthesized by the *de novo* pathway and the salvage pathway through the action of serine palmitoyltransferase and ceramide synthase, respectively (4). Sphingosine kinase (SPHK) 1 and 2, major enzymes in sphingolipid metabolism, catalyze the phosphorylation of sphingosine to generate sphingosine-1-phosphate (S1P). S1P acts as a bioactive molecule to bind to five specific G-protein-coupled receptors (S1P receptors), thus regulating various intracellular signaling pathways during cell proliferation and migration (5-8).

Several pieces of evidence have demonstrated that sphingolipids play crucial roles in regulation of lifespan in model organisms such as worms, flies and yeast (8). These lipid species have also emerged as critical regulators of replicative senescence at the cellular level.

Replicative cellular senescence causes proliferation capacity of cells to become progressively diminished during their repeated replication (9, 10). At this senescent stage, cells lose their replicative potential, leading to gradual impairment of their physiological functions (11). In addition, senescent cells are resistant to diverse stimuli such as mitogenic and apoptotic ones, though they are still viable and metabolically active (12). Generally, senescence triggers morphological changes such as enlarged and flattened cellular shapes and induces a tumor suppressor network involving the ARF/p53 and p16/pRb pathways, which is used as biomarkers to identify the senescent cells (13-15). ARF promotes the stabilization of p53 protein followed by increased expression of p21, thereby contributing to the activation of the p16/pRb pathway. Thus, the interaction between these two tumor suppressor pathways maintains the senescent state of cells (16-18).

Human adipose-derived stromal cells (hAD-SCs) have been proposed as the attractive cell types for cell-based therapies and regenerative medicine. However, hAD-SCs have a drawback related to *in vitro* cell expansion that is the difficulty of generating sufficient numbers of cells for repeated clinical applications, possibly arising from replicative senescence that occurs during continuous cell expansion. To circumvent this cell expansion limitation, we sought to elucidate the molecular mechanisms underlying the diminished proliferation capacity of hAD-SCs. Recent studies have revealed the implication of ceramides or sphingosine in cellular senescence (8). SPHKs have also been shown to

contribute to cell survival, proliferation and resistance to apoptosis (19, 20), though their roles in cellular senescence remain to be investigated.

Mitochondria are essential organelles that generate chemical energy, Adenosine triphosphate (ATP), and their own DNA, mtDNA. In the process of ATP production, reactive oxygen species (ROS) are generated and the ROS can directly oxidize and damage DNA, carbohydrates, proteins, or lipids (81). In general, increased intracellular ROS are eliminated by the antioxidant defense mechanism of two reactive oxygen species (ROS) scavenging enzymes, superoxide dismutase (SOD) and catalase, but ROS could be accumulated in dysfunctional mitochondria. As a result, dysfunctional mitochondria induce diverse diseases including Alzheimer's disease, muscular dystrophy, Lou Gehrig's disease, diabetes, and so on (79), in particular, aging is another essential hallmark of mitochondrial dysfunction (80).

Mitophagy ensures that mitochondria with reduced membrane potential are targeted to nascent autophagic vesicles by tagging them with polyubiquitin chains. Ubiquitylated mitochondria are recognized by a set of receptor proteins which in turn recruit autophagic membranes isolating mitochondria. In this way, mitophagy is a crucial mechanism for the removal of dysfunctional mitochondria and the maintenance of cellular function and viability (83).

In this study, we have found that alteration of sphingolipid profiles and mitochondria functions occur during senescence of hAD-SCs. Notably, both these changes in the levels of sphingolipids and accumulating dysfunctional mitochondria induce cellular senescence are

caused by down-regulated transcription of SPHK1, which is entailed by repeated cell-cycle progression.

MATERIALS AND METHODS

Human adipose-derived stromal cells (hAD-SCs)

Utilization of discarded human tissues for research purposes was approved by the Institutional Review Board (IRB) of Asan Medical center (approval number: 2012-0283). Adipose tissue was obtained from young woman undergoing liposuction. It was treated with 0.075 % collagenase type I (Worthington) in phosphate-buffered saline solution (PBS) for 30 min at 37 °C with gently shaking. Collagenase was inactivated by addition of an equal volume of alpha-minimum essential medium (α -MEM, Gibco) supplemented with 10 % fetal bovine serum (FBS, Gibco) and 1 % penicillin and streptomycin solution (Gibco). This suspension was then centrifuged at 3,000 rpm for 10 min to separate the floating adipocytes from the debris. The cells were plated and incubated in culture medium (α -MEM supplemented with 10 % FBS and 1 % penicillin and streptomycin solution). After 48 h, the non-adherent cells were removed and the adherent cells were washed with PBS. Spindle-shaped cells were obtained by day 4 of culture. Subculture was performed when the cells reached 70-80 % confluence. These cells were maintained at 37 °C in a humidified atmosphere containing 5 % CO₂.

Stable knockdown of SPHK1 and reagents

For stable knockdown of SPHK1, HEK293T cells were transfected with lentiviral packaging vectors as well as SPHK1 shRNA plasmid using electroporation system and after 48 h incubation, SPHK1 shRNA lentiviral particles were obtained. hAD-SCs were infected by adding the lentiviral particles containing SPHK1 shRNA to the culture and then incubated for 48 h. Then, stable clones expressing SPHK1 shRNA were selected by puromycin (2 $\mu\text{g}/\text{ml}$) for 48 h. The stable expression of SPHK1 shRNA was detected by Western blotting analysis. Control and SPHK1-specific shRNAs (Cat. No. HSH055207-1-LVRU6GP and HSH055207-LVRU6P) were acquired from GenecopoeiaTM. The sequences are that shRNA: gcttcgcgccgtagcttta, shSPHK1 #1: ggacctagagagtgagaagta, shSPHK1 #2: ggcgtcatgcatctgttctac, shSPHK1 #3: ggcagcatatggagtatga, shSPHK1-a: GGACCTAGAGAGTGAGAAAGTA, shSPHK1-b: GGCGTCATGCATCTGTTCTAC. Sphingosine kinase inhibitor (Cat. No. 567731) was obtained from Calbiochem. Fumonisin B₁ (Cat. No. F1147) and sphingosine 1-phosphate (Cat. No. S9666) were purchased from Sigma Aldrich.

BrdU incorporation

Proliferation of hAD-SCs was assayed by measuring DNA synthesis using the Cell Proliferation ELISA, BrdU (colorimetric) kit (Roche). Cells were seeded in a 96-well plate at a cell density of 1.0×10^3 cells per well and incubated with BrdU for 4 h at 37 °C. After

removal of BrdU labeling medium, cells were fixed, washed and then quantified for BrdU staining.

Senescence-associated β -galactosidase staining (SA- β -gal staining)

hAD-SCs were plated in 6-well plates at a cell density of 2.0×10^4 cells per well and after 72 h, washed twice with 1 x PBS and then incubated for 15 min at room temperature with fixation solution (0.4 % glutaraldehyde in PBS). Subsequently, cells were washed twice with 1 x PBS and incubated for 16 h at 37 °C with staining solution (X-gal, potassium ferrocyanide and potassium ferricyanide in PBS).

Western blotting

Cells were harvested and homogenized in RIPA buffer containing 1 x Halt protease inhibitor cocktail (Thermo Fisher Scientific) for 30 min on ice. Protein concentration in cell lysates was measured using bicinchoninic acid (BCA) protein assay kit (Thermo Fisher Scientific). The following primary antibodies were used: anti-P-pRb (1:1000), anti-T-pRb (1:1000), anti-P-p53 (1:1000), anti-T-p53 (1:1000), anti-p21 (1:1000), anti-UCP1 (1:1000), anti-P-ULK1 (1:1000), anti-T-ULK1 (1:1000), anti-P-mTOR (1:1000), anti-T-mTOR (1:1000), anti-ATG5 (1:1000), anti-ATG5-12 (1:1000), and anti-SPHK1 (1:1000) antibodies from Cell Signaling Technology and anti- β -Actin (1:10000) and LC3B (1:3000) antibodies from Sigma Aldrich

and anti-timm23 (1:1000) antibody from Abcam and anti-TOM20 (1:3000) and anti- α -tubulin (1:3000) from Santa Cruz Biotechnology.

Quantitative real-time PCR (qRT-PCR)

Total RNA was isolated from hAD-SCs using Trizol (Invitrogen). qRT-PCR was performed on a Bio-Rad (CFX ConnectTM Optics Module) using the TOPrealTM qPCR 2x premix (SYBR Green with low ROX) (Enzynomics) according to the manufacturer's instructions. The sequences of all primers used in qRT-PCR are listed in Table 1.

Liquid chromatography-tandem mass spectrometry (LC-MS/MS) for sphingolipids

For LC-MS/MS, hAD-SCs were seeded in T175 flasks at a cell density of 4×10^5 per flask and incubated for 4 days when the cell density reaches 2.5×10^6 per flask. Cells were dissociated using trypsin-EDTA and subsequently subjected to centrifugation, followed by resuspension of the pelleted cells in cold 80 % methanol. These suspended cells were mixed with sphingolipid internal standard solution and centrifuged at 14,000 rpm for 10 min. Chloroform was added to the resultant supernatant and then the mixture was centrifuged at 2000 g for 15 min. Organic layer was collected and subjected to LC-MS/MS analysis. LC-MS/MS system was equipped with Agilent 1290 HPLC (Agilent) and Qtrap 5500 (ABSciex), and reverse phase column (Pursuit 5 C18 150 \times 2.0 mm) was used. Separation gradient for sphingolipids is as follows; mobile phase A (5 mM ammonium formate/MeOH/

tetrahydrofuran, 500/200/300), mobile phase B (5 mM ammonium formate/MeOH/tetrahydrofuran, 100/200/700), 50 % of A (t = 0 min), 50 % of A (t = 5 min), 30 % of A (t = 8 min), 30 % of A (t = 15 min), 10 % of A (t = 22 min), 10 % of A (t = 25 min), 50 % of A (t = 25.1 min), 50 % of A (t = 30 min) with 200 μ l/min at 35 °C. The MRM (multiple reaction monitoring) mode was used in the positive ion mode and the peak area of the extracted ion chromatogram (EIC) corresponding to the specific transition for each lipid was used for quantitation. Data analysis was performed by using Analyst 1.5.2 software. Calibration range for sphingolipids (ceramide, sphingomyelin, sphinganine and sphingosine) was 0.1-1000 nM ($r^2 \geq 0.99$).

Mitochondrial ROS and Mass

hAD-SCs were seeded in 100 mm dish at a cell density of 2×10^5 per dish and incubated for 3 days. Cells were dissociated using trypsin-EDTA and subsequently subjected to centrifugation, followed by resuspension of the pelleted cells 1X PBS. These cells were then added to 10 μ M solution of MitoSOX™ Red reagent (Invitrogen) and incubated at 37°C for 10 minutes. These suspended cells also were mixed with Mitotracker Green FM (Invitrogen) of 10 nM and incubated at RT for 10 min. And these cells were washed with 1X PBS twice and analyzed by using FACs Calibur instrument (BD Biosciences).

Oxygen consumption rate (OCR)

Measurement of intact cellular respiration was performed using the Seahorse XF24 analyzer. Respiration was measured in the presence of the mitochondrial inhibitor 1.0 µg/ml of oligomycin (Sigma) and 10 µM of the mitochondrial uncoupler FCCP (Sigma) to assess maximal oxidative capacity. Rotenone (Sigma) and antimycin A(Sigma) at 10nM each inhibited mitochondria complex I and III respectively.

NAD assay

Total NAD⁺ and NADH were tested using an NAD⁺/ NADH assay kit (Abcam, ab65348). The 2×10^6 cells were lysed in 400 µl of NAD⁺/NADH extraction buffer, and to detect the NADH in the sample a decomposition step was performed by heating the samples at 60°C for 30 min; under this condition, all the NAD⁺ will be decomposed while NADH will be still intact. The other samples were incubated at room temperature for 5 min to convert NAD⁺ to NADH followed by addition of 10 µl NADH developer into each well and incubated at room temperature for 2 hr. OD was measured at 450 nm using a plate reader.

Glucose uptake and Lactate production

MSCs seeded in 6-well plate at a cell density of 3.0×10^5 per well and incubated for 3 days. The supernatants were collected and diluted to 1:10 and measured by using Glucose uptake colorimetric assay kit (BioVision Inc., K676-100) and Lactate colorimetric assay kit (BioVision Inc., K627-100).

Statistical analysis

All experimental data were analyzed using the GraphPad Prism 5.01 software program (San Diego, CA, USA) and are expressed as the mean \pm standard error (SE) from three independent experiments. $P < 0.05$ was considered statistically significant.

Table 1. Quantitative Real-time PCR (qRT-PCR) primer sequence of sphingolipid metabolic enzymes

Gene		Primer sequences
<i>SPHK1</i>	F	TCCTGGCACTGCTGCACTC
(Sphingosine kinase 1)	R	TAACCATCAATTCCCCATCCAC
<i>SPHK2</i>	F	AGCAGCAGGACCAGAGGCCA
(Sphingosine kinase 2)	R	GGTGAGGGCAAAGCGTGGG
<i>SMS</i>	F	GAAGCCCAACTGCGAAGAATAA
(Sphingomyelin synthase)	R	AGAGTCGCCGAGGGGAATAC
<i>SMase</i>	F	AAGCCCTGCGCACCCCTCAGAA
(Sphingomyelinase)	R	CCTGAAGCTCCCCACCAGCC
<i>CERS2</i>	F	CCGATTACCTGCTGGAGTCAG
(Ceramide synthase 2)	R	GGCGAAGACGATGAAGATGTTG
<i>CERS5</i>	F	GTTTCGCCATCGGAGGAATC
(Ceramide synthase 5)	R	GCCAGCACTGTCGGATGTC
<i>CERS6</i>	F	GGGATCTTAGCCTGGTTCTGG
(Ceramide synthase 6)	R	GCCTCCTCCGTGTTCTTCAG
<i>CDase</i>	F	GATATTGGCCCCAGCCTACTTT
(Ceramidase)	R	ACCCTGCTTAGCATCGAGTTCA
<i>SPT</i>	F	GGTGGAGATGGTACAGGCG
(Serine palmitoyltransferase)	R	TGGTTGCCACTCTTCAATCAG
<i>SPL</i>	F	TGGAGGTGGATGTGCGGGCAA
(Sphingosine-1-phosphate lyase)	R	CCCAGACAAGCGTCGACATGAAG
<i>S1PP</i>	F	CCATTTGTGGACCTGATTGACA
(Sphingosine-1-phosphate phosphatase)	R	ACTTCCTAGTATCTCGGCTGTG
<i>GAPDH</i>	F	TGAACGGGAAGCTCACTG
	R	TCCACCACCCTGTTGCTGTA

RESULTS

Continuous expansion of hAD-SCs induces cellular senescence

To identify the precise molecular mechanisms by which proliferation capacity of hAD-SCs is reduced during *in vitro* cell expansion, we first checked the proliferation rates of these cells undergoing repeated cell division. To this end, we used BrdU incorporation to assay DNA synthesis/cell cycle progression in early (3 or 4 passages)- and late (17 or 18 passages)-passage cells. As expected, hAD-SCs of high passage numbers had a markedly diminished proliferation rate as demonstrated by incorporation of less BrdU into late-passage cells than early-passage cells (Fig. 1A). In line with this, the late-passage cells exhibited a higher activity of senescence-associated- β -galactosidase (SA- β -gal) than the early-passage cells (Fig. 1B, C). Consistently, the levels of cellular senescence markers, including phospho-p53 and p21, were highly enhanced in the late cells, compared to those in the early-passage cells (Fig. 1D). In contrast, the level of phosphorylated pRb, which allows cell cycle progression, was lower in the late-passage cells than in the early cells (Fig. 1D). Together, these results indicate that hAD-SCs undergo cellular senescence during continuous *in vitro* expansion.

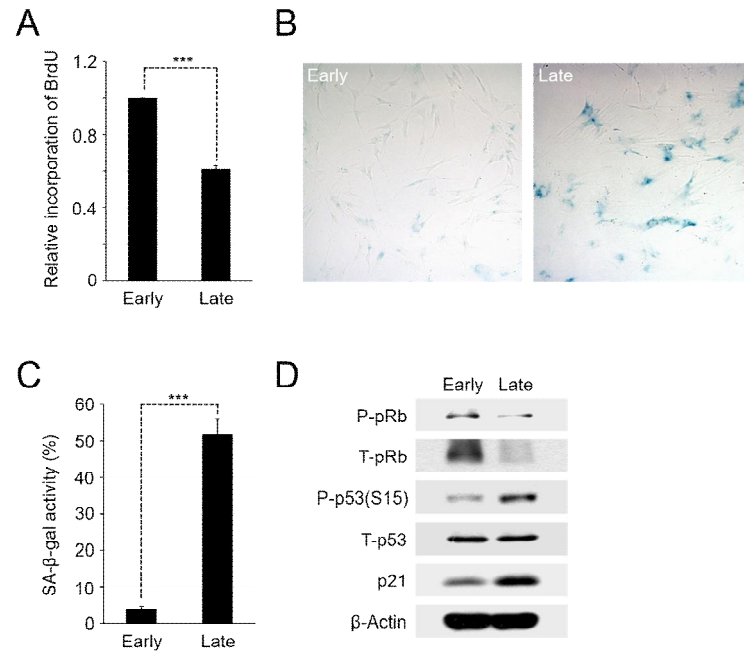


Fig. 1. High passage hAD-SCs undergo cellular senescence. (A) BrdU incorporation assay showing reduced proliferation capacity of late-passage cells relative to early-passage cells. Error bars indicate the standard error (SE). Asterisks above the bars denote *** $P < 0.001$ compared to early-passage cells. (B) Late-passage hAD-SCs display higher activity of senescence-associated- β -galactosidase (SA- β -gal) than early-passage cells. (C) Quantification of activities of SA- β -gal in early- and late-passage hAD-SCs. For this, the number of SA- β -gal positive cells per field was counted. *** $P < 0.001$ (D) Cellular levels of senescence markers, phospho-p53 and p21 are increased in late-passage cells, compared to those in early-passage cells, as analyzed by Western blotting. β -Actin serves as a loading control.

Reduced transcription of SPHK1 in senescent hAD-SCs

The alteration of sphingolipid profiles has been indicated the possibility that the expression and/or activity of sphingolipid metabolic enzymes could be changed in senescent hAD-SCs (78). we next compared the expression levels of several sphingolipid metabolic enzymes in the late-passage cells with those in the early-passage cells. Of note, quantitative RT-PCR analysis revealed that higher passage hAD-SCs have a significantly reduced level of sphingosin kinase 1 (SPHK1) mRNA, compared to that in lower passage ones (Fig. 2A). In contrast, neither SPHK2, an isoform of SPHK1 nor the other key sphingolipid metabolic genes exhibited a marked change in the amount of each transcript as the passage number increases. Consistent with the lowered level of its mRNA, the expression of SPHK1 protein was also highly decreased in the late-passage cells, compared to that in the early-passage cells (Fig. 2B, C). Therefore, these results suggest that transcription of SPHK1 is down-regulated during hAD-SCs senescence.

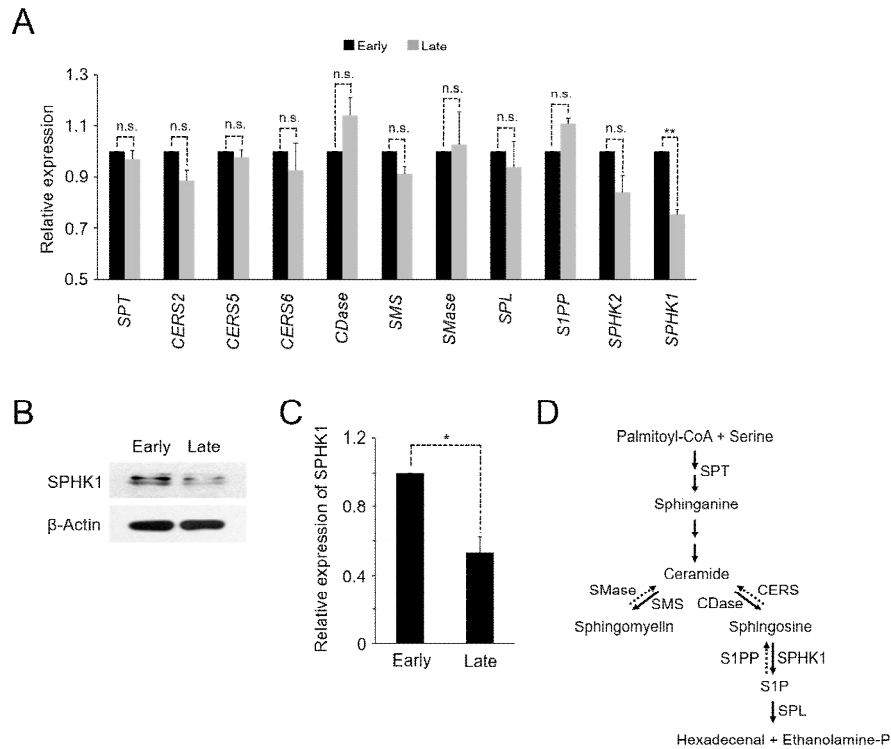


Fig. 2. Transcription of SPHK1 is reduced in senescent hAD-SCs. (A) Late-passage hAD-SCs have lower levels of SPHK1 mRNA than early-passage cells as shown by qRT-PCR. ** $P < 0.01$ compared to early-passage cells. n.s. not significant. (B) Relative expression of SPHK1 protein in early- and late-passage cells. β -Actin is a loading control. (C) Quantification of SPHK1 protein levels in (B) (normalized to β -Actin). * $P < 0.05$. (D) Scheme of sphingolipid metabolism. SPT, serine palmitoyltransferase; SMase, sphingomyelinase; SMS, sphingomyelin synthase; CDase, ceramidase; CERS, ceramide synthase; SPHK1, sphingosine kinase 1; S1PP, sphingosine-1-phosphate phosphatase; SPL, sphingosine-1-phosphate lyase.

Silencing of SPHK1 leads to cellular senescence

Given that SPHK1 is a key regulator of the balance of anti-growth sphingolipids, ceramide and sphingosine and pro-growth sphingolipid, S1P (21), it is possible that down-regulation of SPHK1 transcription might be a critical inducer of cellular senescence in high passage hAD-SCs. To test this possibility, we carried out lentiviral shRNA-mediated silencing of SPHK1 or repressed its enzymatic activity to examine sphingolipid profile and cellular senescence in cells lacking the action of SPHK1. We tested the efficacies of three shRNAs specific for SPHK1 (designated shSPHK1 #1, #2 or #3) by Western blot analysis. Although all three shRNAs silenced SPHK1 (Fig. 3A), we used shSPHK1 #2 for further experiments because it is more effective, compared to the other two shRNAs. To more confirm the characteristics of senescence, we conducted SA- β -gal staining and western blotting in the shCON and shSPHK1 cells (Fig 3C-E). As shown these results, the senescence markers were enhanced and cell proliferation was decreased in the knockdown of SPHK1 (Fig. 3B). Overall, these data support that reduced transcription of SPHK1 is responsible for cellular senescence which are elicited by continuous cell expansion.

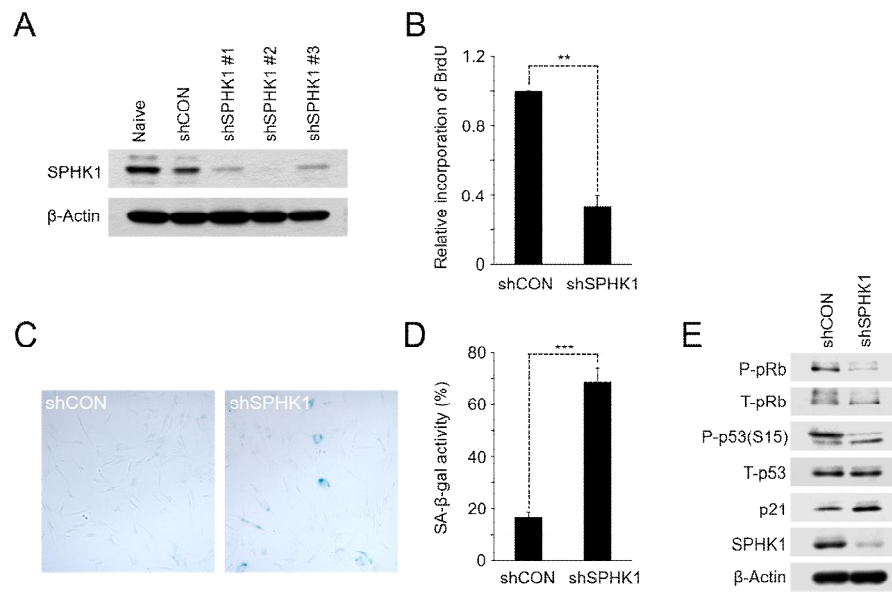


Fig. 3. Knockdown of SPHK1 promotes cellular senescence. (A) Western blotting showing knockdown efficacies of shRNAs against SPHK1 (shSPHK1 #1-3). shCON, a negative control shRNA. (B) Proliferation capacity is decreased in SPHK1-depleted hAD-SCs. $**P < 0.01$ compared to control shRNA-expressing cells. (C) Cellular senescence is enhanced in SPHK1-silenced hAD-SCs as shown by relatively higher activity of SA-β-gal. (D) Quantification of activities of SA-β-gal in shCON or shSPHK1-expressing hAD-SCs. $***P < 0.001$. (E) Depletion of SPHK1 causes increase in the levels of senescence markers. β-Actin serves as a loading control.

Inhibition of enzymatic activity of SPHK1 induces cellular senescence

Knockdown of SPHK1 as well as treatment with SKI, a SPHK1 inhibitor reduced significantly incorporation of BrdU into cellular DNA, compared to that in control cells (Fig. 4A), indicative of the lowered proliferation ability. Like high passage cells, SPHK1-depleted or SKI-treated hAD-SCs underwent accelerated cellular senescence as evidenced by higher activity of SA- β -gal (Fig 4B, C). In support of this, the levels of cellular senescence markers, phospho-p53 and p21 were up-regulated in the SPHK1-silenced or SKI-treated cells with the level of phospho-pRb, a marker of cell proliferation reduced (Fig. 4D). siRNA-mediated silencing of SPHK1 has been shown to induce apoptosis in MCF-7 breast cancer cells (22). Thus, we also checked whether treatment with SKI could induce this programmed cell death in hAD-SCs. In contrast, annexin V staining revealed no significant increase in the number of apoptotic cells in SKI-treated hAD-SCs (Fig. 4E). Thus, it seems likely that down-regulation of SPHK1 expression or activity induces cellular senescence and/or apoptosis depending on the cell types and cell-context.

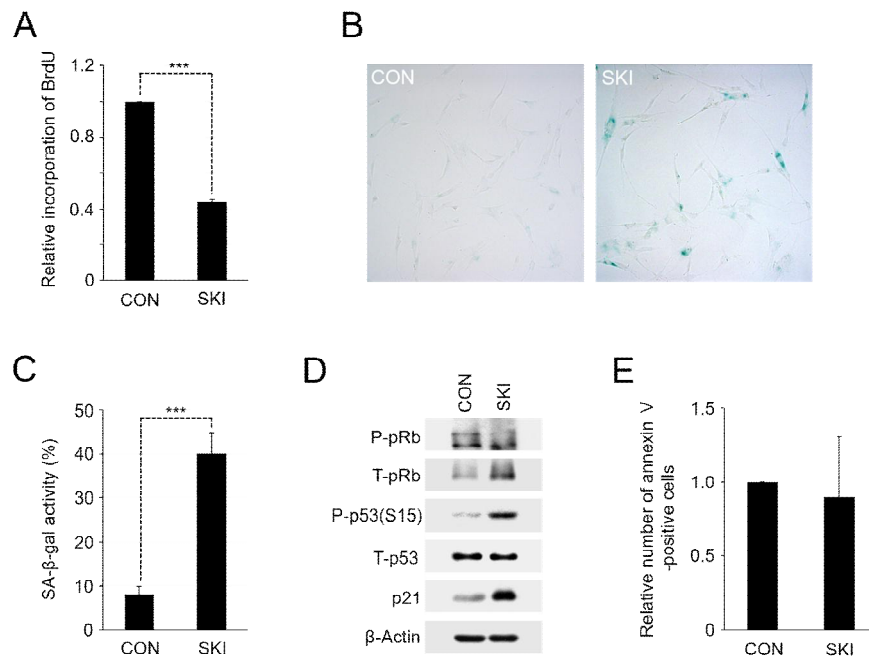


Fig. 4. Inhibition of enzymatic activity of SPHK1 accelerates cellular senescence. (A) Treatment with SKI interferes with proliferation of hAD-SCs. *** $P < 0.001$. (B) Activity of SA-β-gal is augmented by treatment with SKI. (C) Quantification of activities of SA-β-gal in DMSO-treated control (CON) and SKI-treated hAD-SCs. *** $P < 0.001$. (D) hAD-SCs treated with SKI exhibit higher expression levels of senescence markers than control cells. (E) SKI-mediated inhibition of SPHK1 activity does not induce apoptosis in hAD-SCs as assayed by annexin V staining.

Continuous expansion of hAD-SCs leads to accumulation of sphingolipids

Accumulating evidence reveals critical roles of bioactive sphingolipids in mechanism of mammalian cell senescence (8). Thus, we hypothesized that these lipid metabolites could function as potential mediators of hAD-SCs senescence. To test this assumption, we first used liquid chromatography-tandem mass spectrometry (LC-MS/MS) to identify the most abundant subspecies of ceramide and sphingomyelin in hAD-SCs. As shown in Fig. 3A and 3B, C16 ceramide and 16:0 sphingomyelin were found to be the major subspecies in these cells. We next examined whether changes in the cellular levels of sphingolipids including these main subspecies would occur in hAD-SCs, depending on their passage numbers. Importantly, the levels of key sphingolipid species, C16 ceramide, 16:0 sphingomyelin, sphinganine and sphingosine, were significantly higher in the late-passage and shSPHK1 cells than those in the early-passage and control cells (Fig. 5C and D). Taken together, these results suggest that multiple rounds of cell division induce accumulation of anti-growth bioactive sphingolipids, such as ceramide and sphingosine, thereby resulting in replicative senescence in hAD-SCs.

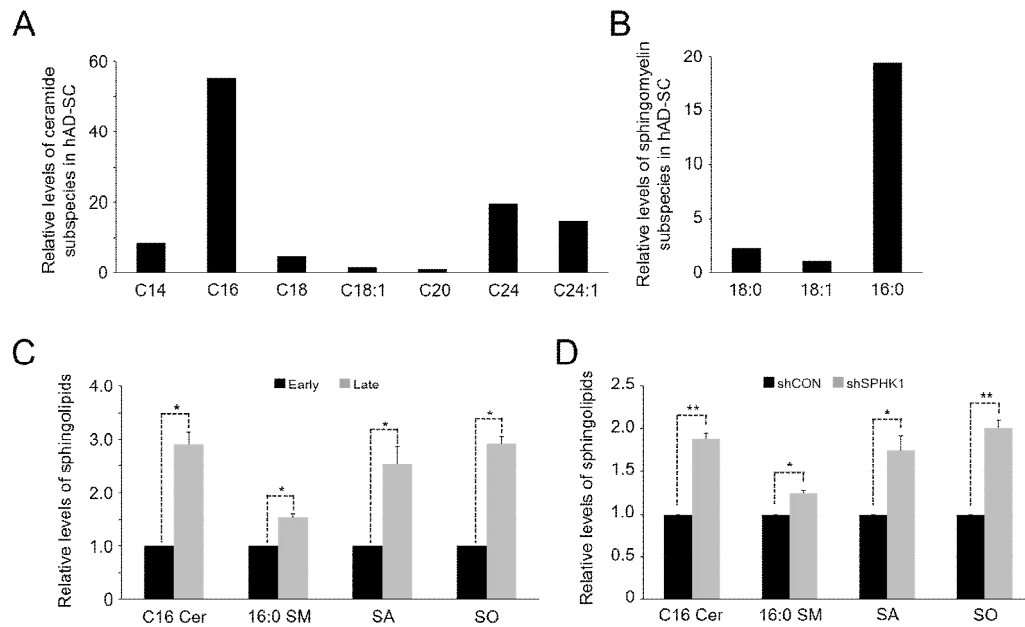


Fig. 5. Senescent hAD-SCs changes in sphingolipid profile. (A, B) LC-MS/MS analysis showing the relative amounts of ceramide (A) and sphingomyelin (B) subspecies in hAD-SCs. (C) Elevation of levels of sphingolipid species in senescent late-passage hAD-SCs. Cer, ceramide; SM, sphingomyelin; SA, sphinganine; SO, sphingosine. * $P < 0.05$ (D) Elevated levels of key sphingolipid species induced by knockdown of SPHK1. * $P < 0.05$ and ** $P < 0.01$, compared to control shRNA-expressing cells.

Inhibition of ceramide synthesis does not attenuate senescence accelerated by SPHK1 knockdown

While ceramide and sphingosine are usually implicated in induction of cell-cycle arrest, apoptosis, and senescence, sphingosine-1-phosphate (S1P) promotes cell proliferation, survival, and migration (23). As shown the Fig 5D, the quantities of ceramide are potently increased in the SPHK1 cells compared to shCON cells. So, we assumed that ceramides enhanced by depletion of SPHK1 could induce cellular aging and we conducted to treat the fumonisin B1 (FB1), a ceramide synthase inhibitor to repress the synthesis of ceramide. BrdU incorporation assays showed that the proliferation impeded by shRNA-mediated silencing of SPHK1 could not be recovered by single treatment with fumonisin B₁ (FB₁) (Fig. 6A). Also, the elevated activity of SA- β -gal in SPHK1-silenced cells could not be reduced by simultaneous co-treatment with FB₁ (Fig. 6B and C). It seems like that the cellular senescence induced by decreasing SPHK1 does not restore inhibiting synthesis of ceramide with treating FB₁.

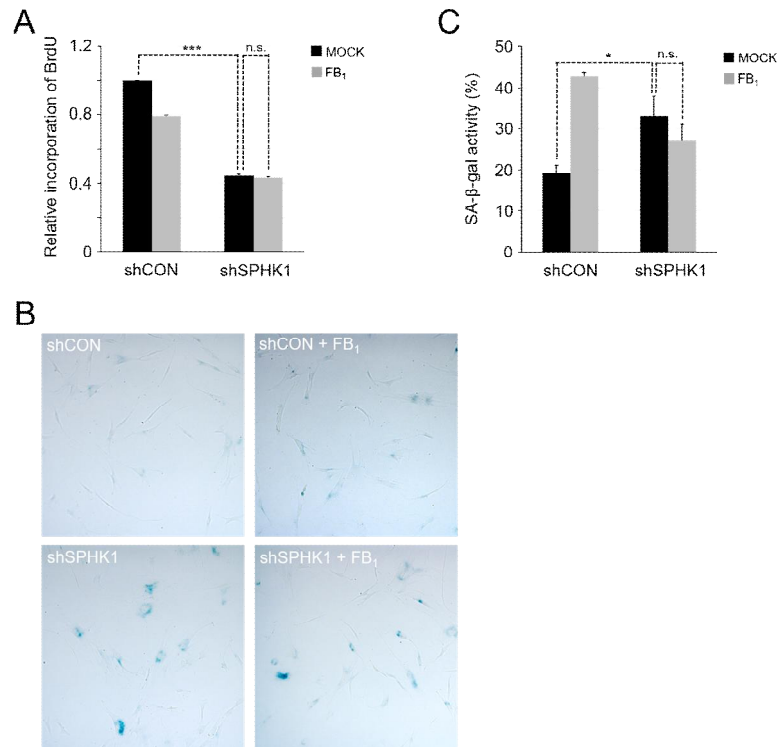


Fig. 6. Single inhibition of ceramide synthesis does not attenuate senescence accelerated by SPHK1 knockdown. (A) Relative proliferation rates of shCON or shSPHK1-expressing hAD-SCs which were treated with FB₁ or not. (B) Increased activity of SA-β-gal in SPHK1-depleted cells is not reversed significantly by single treatment with FB₁. (C) Quantification of activities of SA-β-gal in shCON or shSPHK1-expressing cells which were treated with FB₁ or not. *P<0.05.

Supplementation of S1P does not recover senescence enhanced by SPHK1 knockdown

Expression of a pro-growth sphingolipid, S1P, is decreased by knockdown of SPHK1 according to sphingolipid metabolism. So, we estimated that supplementation of S1P could recover the cellular senescence enhanced by inhibiting SPHK1. But shSPHK1 cells as well as treatment with S1P decreased considerably incorporation of BrdU into cellular DNA, compared to that in shCON cells (Fig 7A). Also, SPHK1-depleted hAD-SCs reached rapid cellular senescence as evidenced by higher SA- β -gal activity (Fig 7B, C). Like as the result of BrdU incorporation, the exogenous addition of S1P did not recover enhanced cellular senescence induced in SPHK1-silenced cells. Taking together, we conclude that cellular senescence induced by depletion of SPHK1 does not recover by S1P treatment alone.

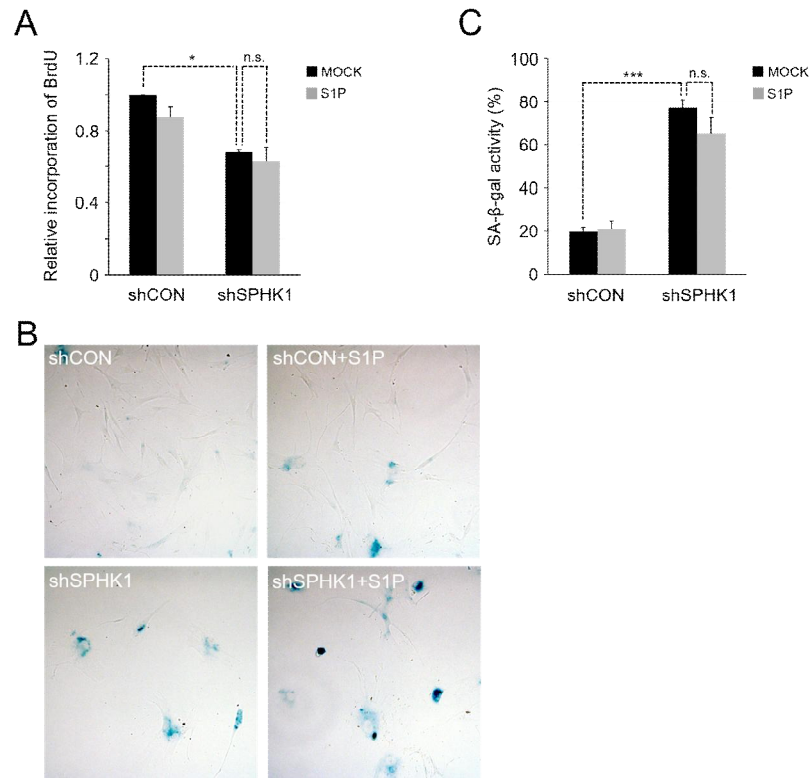


Fig. 7. Single supplementation of S1P does not recover senescence enhanced by SPHK1 knockdown. (A) Relative proliferation capacities of shCON or shSPHK1-expressing hAD-SCs which were treated with S1P or not. * $P < 0.05$. (B) Enhanced cellular senescence of SPHK1-silenced cells is not reverted by exogenous addition of S1P as assayed by SA-β-gal activity. (C) Quantification of activities of SA-β-gal in shCON or shSPHK1-expressing cells which were supplemented with S1P or not. *** $P < 0.001$ compared to control shRNA-expressing cells.

Alteration of sphingolipid profiles causes cellular senescence in SPHK1-depleted cells

We speculated that the cellular senescence accelerated by SPHK1 knockdown might be influenced by both increasing ceramide levels and decreasing S1P levels. To test this hypothesis, we investigated whether SPHK1 knockdown-induced cellular senescence could be attenuated by inhibition of ceramide synthesis and exogenous supplementation of S1P during cell culture. BrdU incorporation assays showed that the proliferation impeded by shRNA-mediated silencing of SPHK1 could not be recovered by co-treatment with S1P and fumonisin B₁ (FB₁) (Fig. 8A), indicating the irreversibility of cellular senescence. In contrast, the elevated activity of SA- β -gal in SPHK1-silenced cells could be reduced by simultaneous co-treatment with S1P and FB₁ (Fig. 8B, C), suggesting that cellular senescence accelerated by SPHK1 depletion may result from increase in ceramide levels with concurrent decrease in S1P levels. Taking together, we conclude that depletion of SPHK1 alters the balance of pro-death and anti-death bioactive sphingolipids, enhancing replicative cellular senescence.

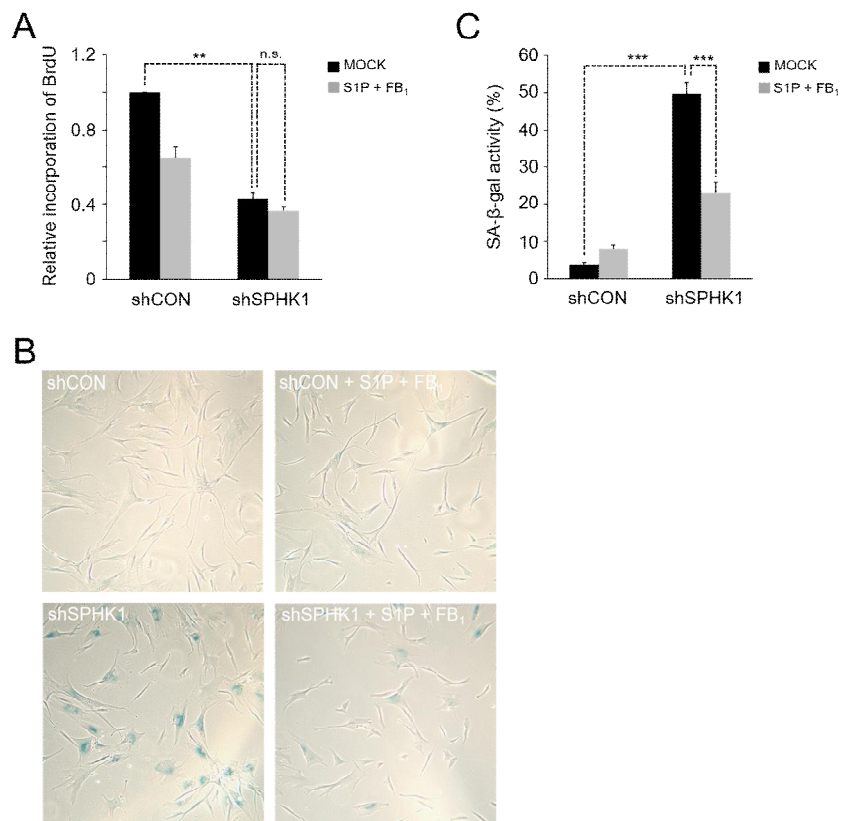


Fig. 8. SPHK1 knockdown-accelerated cellular senescence is attenuated by inhibition of ceramide synthesis and concurrent supplementation of S1P. (A) No rescue of reduced proliferation capacity of SPHK1-depleted hAD-SCs by co-treatment with S1P and FB₁. **P<0.01. (B) Co-treatment with S1P and FB₁ lowers the activity of SA-β-gal enhanced by depletion of SPHK1. (C) Quantification of activities of SA-β-gal in shCON or shSPHK1-expressing hAD-SCs which were co-treated with S1P and FB₁ or not. ***P<0.001.

The shRNA-mediate silencing SPHK1 enhances glycolysis and OCR

Mitochondria are fascinating structures that generate energy and have a central role in energy metabolism. Also, the mitochondria mediate reactive oxygen species (ROS) genesis, cell apoptosis, and calcium (74). Recent researches have been uncovered that alterations of sphingolipids such as ceramides or S1P relate to dysfunctional mitochondria (82). Oxygen Consumption Rate (OCR) is an indicator of mitochondrial function and many studies have shown that OCR level is increased in the mitochondrial unhealthy state. First of all, we examined the energy metabolism in shSPHK1 cells to check how shSPHK1 cells gain the energy (Fig. 9A). The result shown that the glucose uptake and production of lactate are increased in the shSPHK1 cells compared to shCON cells, supporting that energy metabolism changes towards glycolysis in silencing SPHK1 cells. Additionally, we conducted OCR analysis (Fig. 9B-D). First oligomycin, an inhibitor of mitochondrial ATP synthase, is injected and a proton ionophore (uncoupler) such as FCCP is used to estimate the maximal potential respiration sustainable by the cells. Finally, OCR analysis finished following the respiratory chain is inhibited with antimycin A and rotenone to determine the extent of non-mitochondrial oxygen-consuming processes. As a result, the overall OCR was increased, especially, the basal and maximal respiration and proton leak were all increased in shSPHK1 cells compared to shCON cell. Hereby, we concluded that the knockdown of SPHK1 increases all of glycolysis and OCR.

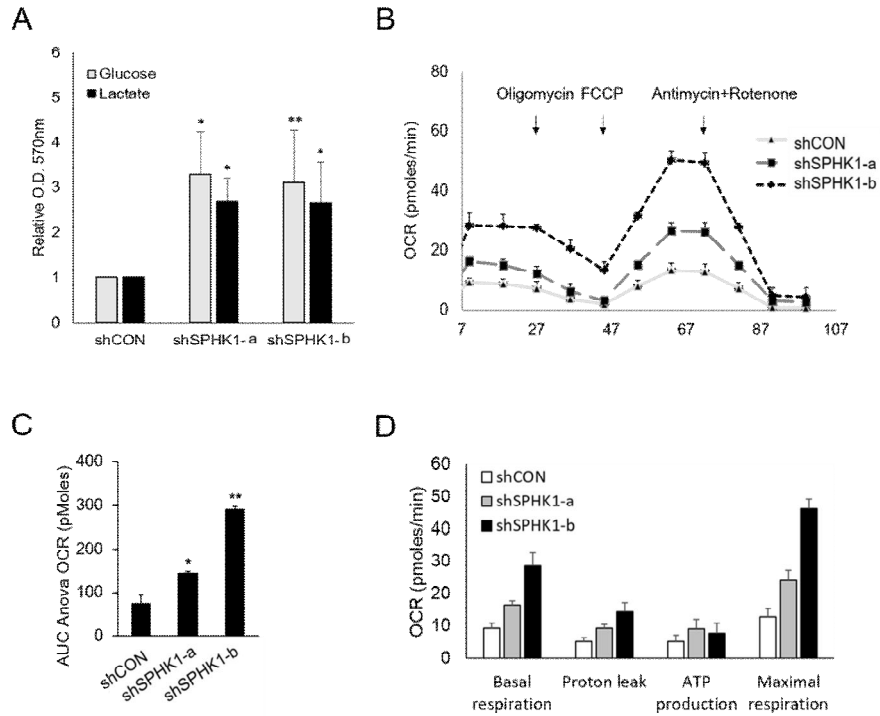


Fig. 9. Depletion of SPHK1 enhances glycolysis and OCR. (A) Metabolic change occurs towards glycolysis in the shSPHK1 cells. Absorbance was measured at O.D. 570nm. All of the shSPHK1-a and -b cells were increased glucose uptake and lactate production compared to shCON cells. * $P < 0.05$ and ** $P < 0.01$ (B) Basal OCR measurements were made followed by injection of oligomycin (1 mg/mL), FCCP (10 μ M), antimycin A (10 μ M) and Rotenone (10 μ M) were injected. (C) Overall OCR was significantly increased in the SPHK1-silenced cells compared to control-silenced cells. (D) Basal respiration, proton leak, ATP production, and maximal respiration were all increased in shSPHK1 cells.

Depletion of SPHK1 induces mitochondrial dysfunction and uncoupling process

We assumed that there is a problem in the process of obtaining energy through the increase of OCR and glycolysis in shSPHK1 cells. To test the mitochondrial ROS level, we investigated flow cytometry analysis in the shCON and shSPHK1 cells. These cells were stained with Mitotracker-Green (MTGR), to measure mitochondria mass, and MitoSOX-Red to indicate mitochondrial ROS production. We indicated that the ROS level is MitoSOX-Red/MTGR stats and the figures have shown (Fig. 10A), as predicted, that powerfully increased in the SPHK1-silenced cells compared with control-silenced cells. The unusual thing is the NAD⁺/NADH ratio (Fig. 10B), as well as mitochondrial ROS and OCR (Fig. 9C), were increased, but ATP production was no corresponding increase. So, we expected that the mitochondrial uncoupling might be induced and checked UCP1 as a representative uncoupling marker. As expected, the expression of that was increased in SKI treated cells (Fig. 10C). Taken together, we concluded that the knockdown of SPHK1 induces mitochondrial ROS and uncoupling process.

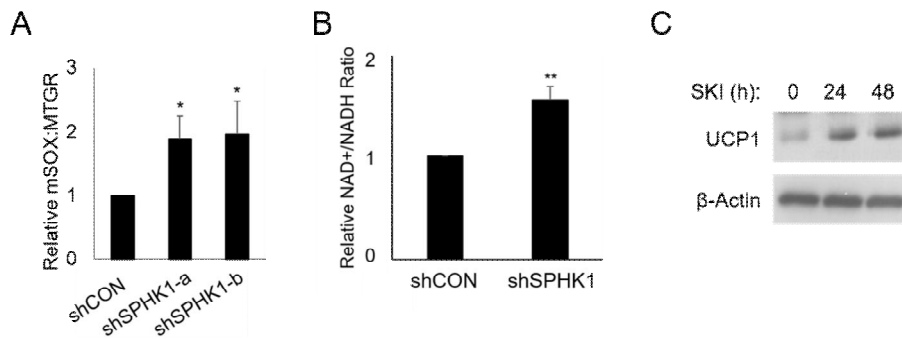


Fig. 10. Depletion of SPHK1 induces mitochondrial dysfunction and uncoupling process.

(A) Mitochondrial ROS was enhanced in the shSPHK1 cells. Mitotracker-Green (MTGR), to measure mitochondria mass, and MitoSOX-Red to indicate mitochondrial ROS production and ROS level represents mitoSOX-Red/MTGR stats. *P<0.05 compared to control shRNA-expressing cells. (B) NAD⁺/NADH ratio also increased in the knockdown of SPHK1.

**P<0.01 (C) UCP1, representative protein of mitochondrial uncoupling process, is

increased in SKI treated cell.

SPHK1 exists in the mitochondria and has an effect on the decrease of autophagy flux

The latest research uncovered that SPHK1 is targeted to mitochondria in the mitochondrial unfolded protein response (UPR^{mt}) (75). FCCP, mitochondrial oxidative phosphorylation uncoupler, disrupts ATP synthesis and induces mitochondrial dysfunction. To check SPHK1 associates with mitochondria in MSCs, we confirmed expression of SPHK1 in the mitochondria after triggering mitochondrial stress using FCCP. We performed mitochondrial fractionation in order to check with accuracy, and the results have shown that SPHK1 exists in mitochondria of control cells (Fig. 11A). Besides, the level of SPHK1 in mitochondria is gradually decreased and LC3 conversion induced in the mitochondrial stress condition induced by FCCP. Of many pieces of research about the relationship between SPHK1 and autophagy, Megan M. Young et al., uncovered that SPHK1 is involved in the endolysosomal trafficking in autophagy (84). In a recent autophagy review, Malene Hansen et al., have shown the autophagy progression as initiation, nucleation, autophagosome maturation, and autophagolysosome (85) (Fig. 11B). So, we have referred to this figure and confirmed the expression of proteins related to the initiation and nucleation step in the knockdown of SPHK1 (Fig 11C). As shown in the result, the activity of mTOR and ULK1 as initiation step markers differ in shSPHK1-a and -b cells, but the expression of ATG5-12 conjugated form was distinctly decreased in all of the shSPHK1 cells compared to shCON cells. Through the results that knockdown of SPHK1 induces accumulating dysfunctional mitochondria,

SPHK1 exists in mitochondria and degrades with mitochondria in condition with inducing mitophagy through treating FCCP, we supposed that SPHK1 is involved in autophagy and mitophagy. The recent many researches have been reported about relation between SPHK1 and autophagy (76, 77). Autophagy is an intracellular lysosome-mediated degradation system that damaged cells are clean out and maintains cellular homeostasis and functions. Rapamycin is autophagy inducer because the inhibitory effect of that on the mTOR activity and Bafilomycin A1 is an inhibitor of autophagy flux by inhibiting fusion of autophagosome. We examined the autophagy flux in shRNA-mediated silencing SPHK1 to confirm the relationship between SPHK1 and autophagy. The data have shown that LC3B level was already highly expressed in the basal level and overall autophagy flux was decreased in shSPHK1 cells compared to shCON cells (Fig. 11D). Based on this result, we have concluded that SPHK1 exists in the mitochondria and is associated with ATG5-12 conjugated formation in the autophagy initiation step and has an effect on the removal of dysfunctional mitochondria with decreasing autophagy flux.

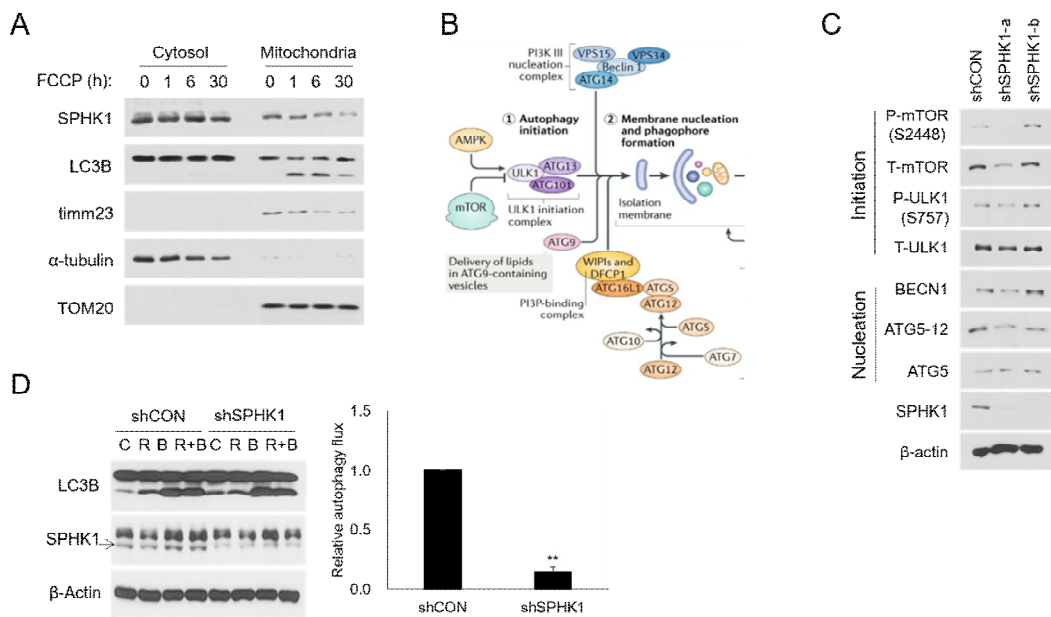


Fig. 11. SPHK1 exists in the mitochondria. (A) The conversion of LC3, as representative autophagy markers, induced in mitochondria. And timm23 as mitochondria marker is corresponding decreasing. These cells were treated with FCCP at 10uM for time-dependent. The α -tubulin represents cytosol protein, Tom20 indicates mitochondrial protein and loading control. (B) The scheme that the Nature Reviews Molecular Cell Biology volume 19, pages 579-593 (2018) referred to has shown autophagy progression. (C) The expression of mTOR and ULK1 related to the initiation step differ in shSPHK1-a and -b cells but the expression of ATG5-12 conjugated form is decreased in all of the shSPHK1 cells compared to shCON cells. (D) Western blotting showing knockdown efficacies of shRNAs against SPHK1 (shSPHK1 #2) and expression of LC3B, representative autophagy markers in the shSPHK1 and shCON cells. Knockdown of SPHK1 reduces the autophagy flux. **P<0.1.

DISCUSSION

Recent studies have demonstrated that sphingolipids, such as ceramide and sphingosine, and their metabolic enzymes are involved in regulation of cellular senescence in various cell types (8). However, it remains elusive how changes in the levels of sphingolipid species and in the activities of their metabolic enzymes are induced in cells undergoing replicative senescence. In this study, we have shown that down-regulation of SPHK1 expression at the transcriptional level acts as a key inducer of altered sphingolipid profiles, thereby accelerating cellular senescence during cell expansion. Like most of human cell types, human adipose tissue-derived stromal cells (hAD-SCs), a model of replicative senescence used in this work, exhibited a decrease in proliferation capacity with concomitant enhancement of cellular senescence as they undergo increasing numbers of passages. Previously, human senescent fibroblasts of high passage numbers were shown to have increased ceramide levels and sphingomyelinase (SMase) activity, compared to ones of lower passage numbers (5). It is of note that the senescent hAD-SCs of high passage numbers have significantly elevated levels not only of ceramide but of other sphingolipids including sphingomyelin, sphingosine and sphinganine (Fig. 1). In addition, among several sphingolipid metabolic enzymes, expression of SPHK1 only was significantly down-regulated at the mRNA level as well as the protein level in the senescent hAD-SCs. In

support of pivotal role for this decreased expression of SPHK1 in inducing senescence, shRNA-mediated silencing of SPHK1 promoted cellular senescence at the expense of proliferation and up-regulated the levels of the same sphingolipid species as observed in late-passage cells. Pharmacological inhibition of SPHK1 activity also suppressed cell growth but accelerated cellular senescence. Furthermore, the enhanced cellular senescence in SPHK1-depleted cells could be attenuated by exogenous addition of S1P with concurrent inhibition of ceramide synthesis. Given these findings, it is possible that reduced transcription of SPHK1 may function as a bona fide inducer of replicative senescence by regulating sphingolipid metabolism during repeated rounds of cell division.

Cellular levels of SPHK1 expression have been shown to play key roles in sphingolipid-mediated determination of cell fates. The levels of SPHK1 mRNA are generally increased in various types of human cancers (24). In line with this, overexpression of SPHK1 promotes focus formation, growth of cells in soft agar and tumor formation in NOD/SCID mice (25), pointing to its oncogenic role but reduces cellular apoptosis (26). Increased levels of S1P by overexpression of SPHK1 also expedite cell-cycle progression and enhance cell growth, whereas overexpression of S1P phosphatase increases cell death (27). Thus, it appears that up-regulation of SPHK1 expression leads to pro-growth and anti-apoptotic signals mediated by the SPHK1/S1P pathway. Down-regulation of SPHK1 expression provides a mechanism of tumor suppression by modulating the levels of sphingolipid species as evidenced by analysis of double-KO mice lacking a tumor suppressor p53 and SPHK1. p53-null mice

develop thymic lymphomas, which were completely abrogated by deletion of SPHK1 in these mice (28). In p53-KO mice, expression of SPHK1 and levels of S1P are elevated, whereas levels of ceramide are decreased, compared to wild-type mice. These sphingolipid profiles in p53-null mice are reversed by deletion of SPHK1, in turn accompanied by cellular senescence but not by apoptosis. Notably, SPHK1 has been shown to undergo proteolytic degradation in response to genotoxic stress in a p53-dependent manner (29). These results suggest that p53 induces its tumor suppressor effects by down-regulating expression of SPHK1 at the posttranslational level, leading to decreased levels of S1P and increased levels of ceramide and sphingosine, which then mediate cellular senescence. As shown in our results, down-regulation of SPHK1 expression at the transcriptional level causes similarly elevation of ceramide and sphingosine levels, contributing to replicative cellular senescence. Given these results, it is tempting to speculate that mode of regulation of SPHK1 expression to induce cellular senescence depends on upstream inducers and physiological context. It seems likely that for tissue homeostasis, a rapid response mechanism for inducing senescence, such as p53-mediated proteolysis of SPHK1, is necessary for cells to prevent immediately tumorigenesis in response to genotoxic stresses including DNA damage-inducing agents and oncogenic activation. In contrast, a relatively slower mechanism, such as down-regulation of SPHK1 transcription, may be appropriate for inducing replicative senescence in response to telomere shortening and oxidative stress entailed by multiple rounds of cell division. However, it cannot be excluded that both the rapid and slow

mechanisms might function in parallel for preventing tumor formation and/or inducing replicative senescence. A few modes of regulation would ensure a robust mechanism to induce cellular senescence in the right place at the right time during tissue homeostasis and aging.

As sphingolipid species, including sphingomyelin, ceramide, sphingosine and S1P, are interconvertible, knockdown of one sphingolipid metabolic enzyme would alter relative levels of these metabolites. Furthermore, the levels of activity of a sphingolipid metabolic enzyme could affect those of other enzymes. Overexpression of S1P phosphatase-1, which dephosphorylates S1P, enhances *de novo* synthesis of ceramide, possibly owing to de-repression of serine palmitoyltransferase or ceramide synthase by S1P (21). Treatment with fumonisin B₁, an inhibitor of ceramide synthase, has been shown to increase the activity of acidic sphingomyelinase, accompanied with a decrease of sphingomyelin, and the expression and activities of serine palmitoyltransferase and SPHK1 in mouse liver (30). Thus, ‘sphingolipid rheostat’ has been proposed to regulate relative levels of sphingolipid metabolites, thereby determining cell fates (21). SPHK1 acts as a critical regulator of sphingolipid rheostat to maintain a balance between pro-growth and pro-death bioactive sphingolipids. As shown by our assays, knockdown of SPHK1 seemed to tilt the balance of ceramide, sphingosine and S1P in favor of growth inhibition and cell death. SPHK1 knockdown-reduced proliferation capacity could be recovered by neither co-treatment with both S1P and a ceramide synthesis inhibitor, fumonisin B₁ nor single treatment with

either one, indicative of the irreversibility of cellular senescence accelerated by depletion of SPHK1. However, this cellular senescence could be attenuated efficiently by co-treatment with both the reagents but not by treatment with either one, suggesting the crucial roles that increased ceramide levels and decreased S1P levels each play in promoting replicative senescence in SPHK1-depleted cells. In most cell types, the cellular levels of ceramide, sphingosine and S1P differ approximately by an order of magnitude, with ceramide being present at the highest and S1P at the lowest level (2). A small change in ceramide can lead to profound changes in S1P. In addition, the levels of ceramide in SPHK1-depleted cells are about two times higher than those in normal control cells. Despite these facts, inhibition of ceramide generation alone was unable to attenuate acceleration of cellular senescence by knockdown of SPHK1, thus revealing the strong potency of low levels of S1P in shifting the balance between pro- and anti-death signals toward cell survival.

In this study, we confirmed the correlation between cellular senescence induced by depletion of SPHK1 and mitochondrial dysfunction. The knockdown of SPHK1 induced enhancing mitochondrial OCR and NAD/NADH⁺ ratio, but ATP production is no significant increase in this situation. That's why mitochondrial ROS and proton leak, as well as overall OCR, is enhanced, so we have an assumption that proceeds with mitochondrial uncoupling. The UCP1 as representative uncoupling marker was highly increased in SKI treated cell. The representative degradation mechanism of dysfunctional mitochondria is mitophagy. Megan M. Young et al., uncovered that SPHK1 is involved in the endolysosomal trafficking in

autophagy (84). So, we confirmed the stepwise autophagy flux, the result has been shown the autophagy nucleation step is blocked in shSPHK1 hAD-SCs, unlike ref. 84. We need further research but these results have suggested that SPHK1 is associated with autophagy flux related to ATG5-12 conjugated formation in the autophagy initiation step, and has an effect on the removal of dysfunctional mitochondria.

Based on all these results, this study has found that down-regulation of SPHK1 transcription serve as a critical inducer of a tilt in the balance between pro- and anti-growth bioactive sphingolipids in favor of growth inhibition and cellular senescence during *in vitro* cell expansion. Further studies are warranted to elucidate the molecular mechanisms by which SPHK1 expression is regulated negatively at the transcriptional level during multiple rounds of cell divisions. Since SPHK1 is an essential regulator of sphingolipid rheostat and mitochondria healthy, better understanding of control of its expression holds promise to develop novel tools to prolong the proliferation capacity of cells for cell-based therapy and regenerative medicine.

REFERENCES

1. Jaiswal N, Haynesworth SE, Caplan AI, Bruder SP. Osteogenic differentiation of purified, culture-expanded human mesenchymal stem cells in vitro. *J Cell Biochem* 1997;64(2):295-312.
2. Li J, Pei M. Cell senescence: a challenge in cartilage engineering and regeneration. *Tissue Eng Part B Rev* 2012;18(4):270-87.
3. Sakaguchi Y, Sekiya I, Yagishita K, Muneta T. Comparison of human stem cells derived from various mesenchymal tissues: superiority of synovium as a cell source. *Arthritis Rheum* 2005;52(8):2521-9.
4. Choong PF, Mok PL, Cheong SK, Leong CF, Then KY. Generating neuron-like cells from BM-derived mesenchymal stromal cells in vitro. *Cytherapy* 2007;9(2):170-83.
5. Wong CY, Cheong SK, Mok PL, Leong CF. Differentiation of human mesenchymal stem cells into mesangial cells in post-glomerular injury murine model. *Pathology* 2008;40(1):52-7.
6. Jin HJ, Bae YK, Kim M, Kwon SJ, Jeon HB, Choi SJ, Kim SW, Yang YS, Oh W, Chang JW. Comparative analysis of human mesenchymal stem cells from bone

- marrow, adipose tissue, and umbilical cord blood as sources of cell therapy. *Int J Mol Sci* 2013;3;14(9):17986-8001.
7. HAYFLICK L. THE LIMITED IN VITRO LIFETIME OF HUMAN DIPLOID CELL STRAINS. *Exp Cell Res* 1965;37:614-36.
 8. Campisi J. The biology of replicative senescence. *Eur J Cancer* 1997; 33(5):703-9.
 9. Loo DT, Fuquay JI, Rawson CL, Barnes DW. Extended culture of mouse embryo cells without senescence: inhibition by serum. *Science* 1987; 10;236(4798):200-2.
 10. Sherr CJ, DePinho RA. Cellular senescence: mitotic clock or culture shock? *Cell* 2000;18;102(4):407-10.
 11. L. Hayflick, P.S. Moorhead. The serial cultivation of human diploid cell strains. *Exp. Cell Res* 1961;25: 585–621.
 12. V. Chaturvedi, et al. Apoptosis in proliferating, senescent, and immortalized keratinocytes. *J. Biol. Chem* 1999;274:23358–23367.
 13. R. Marcotte, C. Lacelle, E. Wang. Senescent fibroblasts resist apoptosis by downregulating caspase-3. *Mech. Ageing Dev* 2004;125:777-783.
 14. Horikawa I, Fujita K, Jenkins LM, Hiyoshi Y, Mondal AM, Vojtesek B, Lane DP, Appella E, Harris CC. Autophagic degradation of the inhibitory p53 isoform $\Delta 133p53\alpha$ as a regulatory mechanism for p53-mediated senescence. *Nat Commun.* 2014; 5:4706.

15. Young AR, Narita M, Ferreira M, Kirschner K, Sadaie M, Darot JF, Tavaré S, Arakawa S, Shimizu S, Watt FM, Narita M. Autophagy mediates the mitotic senescence transition. *Genes Dev.* 2009; 23(7):798-803.
16. Grégory Lavieu, Francesca Scarlatti, Giusy Sala, Stéphane Carpentier, Thierry Levade, Riccardo Ghidoni, Joëlle Botti and Patrice Codogno. *J. Biol. Chem.* 2006, 281:8518-8527.
17. Vladimir Beljanski, Christian Knaak, and Charles D. Smith. A Novel Sphingosine Kinase Inhibitor Induces Autophagy in Tumor Cells. *THE JOURNAL OF PHARMACOLOGY AND EXPERIMENTAL THERAPEUTICS.* vol. 333 no. 2 454-464
18. Kummetha Venkata J, An N, Stuart R, Costa LJ, Cai H, Coker W, Song JH, Gibbs K, Matson T, Garrett-Mayer E, Wan Z, Ogretmen B, Smith C, Kang Y. Inhibition of sphingosine kinase 2 down-regulates the expression of c-Myc and Mcl-1 and induces apoptosis in multiple myeloma. *Blood.* 2014-03-559385.
19. Madhunapantula SV1, Hengst J, Gowda R, Fox TE, Yun JK, Robertson GP. Targeting sphingosine kinase-1 to inhibit melanoma. *Pigment Cell Melanoma Res.* 2012 ;25(2):259-74.
20. Kohama, T., A. Olivera, L. Edsall, M.M. Nagiec, R. Dickson, and S. Spiegel. 1998. Molecular cloning and functional characterization of murine sphingosine kinase. *J. Biol. Chem.*273:23722–23728.

21. Liu, H., M. Sugiura, V.E. Nava, L.C. Edsall, K. Kono, S. Poulton, S. Milstien, T. Kohama, and S. Spiegel. 2000. Molecular cloning and functional characterization of a novel mammalian sphingosine kinase type 2 isoform. *J. Biol. Chem.* 275:19513–19520.
22. Bligh, E.G. and Dyer, W.J., A rapid method for total lipid extraction and purification, *Can. J. Biochem. Physiol.* 1959, 37:911-917
23. Codogno P, Meijer AJ. Autophagy and signaling: their role in cell survival and cell death. *Cell Death Differ.* 2005; 12 Suppl 2:1509-18.
24. Mizushima N, Komatsu M. Autophagy: renovation of cells and tissues. *Cell.* 2011;147(4):728-41.
25. Kroemer G, Marino G, Levine B. Autophagy and the integrated stress response. *Mol Cell* 2010; 40: 280–293.
26. Levine B, Mizushima N, Virgin HW: Autophagy in immunity and inflammation. *Nature.* 2011;469:323–35.
27. Levine B, Kroemer G: Autophagy in the pathogenesis of disease. *Cell.* 2008;132:27–42.
28. Mizushima N, Levine B, Cuervo AM, Klionsky DJ: Autophagy fights disease through cellular self-digestion. *Nature.* 2008;451:1069–75.
29. R.J. Youle, D.P. Narendra Mechanisms of mitophagy *Nat. Rev. Mol. Cell Biol.*, 12 (2011), pp. 9–14.

30. Scarlatti F, Granata R, Meijer AJ, Codogno P. Does autophagy have a license to kill mammalian cells? *Cell Death Differ.* 2009;16(1):12-20.
31. Levine B, Yuan J. Autophagy in cell death: an innocent convict? *J Clin Invest.* 2005;115(10):2679-88.
32. Jacinto E and Hall MN. Tor signalling in bugs, brain and brawn. *Nat. Rev. Mol. Cell Biol.* 2003; 4: 117–126
33. Bergamini E, Cavallini G, Donati A and Gori Z. The role of macroautophagy in the ageing process, anti-ageing intervention and age-associated diseases. *Int. J. Biochem. Cell Biol.* 2004;36: 2392–2404
34. Gerland LM, Peyrol S, Lallemand C, Branche R, Magaud JP, Ffrench M. Association of increased autophagic inclusions labeled for beta-galactosidase with fibroblastic aging. *Exp Gerontol.* 2003;38:887–95.
35. Patschan S, Chen J, Polotskaia A, Mendeleev N, Cheng J, Patschan D, et al. Lipid mediators of autophagy in stress-induced premature senescence of endothelial cells. *Am J Physiol Heart Circ Physiol.* 2008;294:H1119–29.
36. Li L, Zhu YQ, Jiang L, Peng W. Increased autophagic activity in senescent human dental pulp cells. *Int Endod J.* 2012; 45(12):1074-9.
37. Young AR, Narita M, Ferreira M, Kirschner K, Sadaie M, Darot JF, Tavaré S, Arakawa S, Shimizu S, Watt FM, Narita M. Autophagy mediates the mitotic senescence transition. *Genes Dev.* 2009; 23(7):798-803.

38. G. E. Palade. An electron microscope study of the mitochondrial structure. *Journal of Histochemistry and Cytochemistry*. vol. 1, no. 4, pp. 188–211, 1953.
39. Saverio Marchi, Carlotta Giorgi, Jan M. Suski, Chiara Agnoletto, Angela Bononi, Massimo Bonora, Elena De Marchi, Sonia Missiroli, Simone Patergnani, Federica Poletti, Alessandro Rimessi, Jerzy Duszynski, Mariusz R. Wieckowski, and Paolo Pinton. Mitochondria-Ros Crosstalk in the Control of Cell Death and Aging. *Journal of signal transduction* volume 2012; article ID 329635, 17 pages.
40. G. C. Brown. Control of respiration and ATP synthesis in mammalian mitochondria and cells. *Biochemical Journal*. 1992;284(1):1-13.
41. A. J. Kowaltowski, N. C. de Souza-Pinto, R. F. Castilho, and A. E. Vercesi. Mitochondria and reactive oxygen species. *Free Radical Biology and Medicine*. 2009;47(4): 333-343.
42. Y. Liu, G. Fiskum, and D. Schubert. Generation of reactive oxygen species by the mitochondrial electron transport chain. *Journal of Neurochemistry*. 2002;80(5): 780-787.
43. J. F. Turrens. Mitochondrial formation of reactive oxygen species. *Journal of Physiology*. 2003;552(2): 335-344.
44. E. Verdin, M. D. Hirschey, L. W. S. Finley, and M. C. Haigis. Sirtuin regulation of mitochondria: energy production, apoptosis, and signaling. *Trends in Biochemical Sciences*. 2010;35(12):669-675

45. S. E. Schriner, N. J. Linford, G. M. Martin et al., Extension of murine life span by overexpression of catalase targeted to mitochondria. *Science*. 2005;308(5730):1909-1911.
46. V. I. Pérez, C. M. Lew, L. A. Cortez et al., Thioredoxin 2 haploinsufficiency in mice results in impaired mitochondrial function and increased oxidative stress. *Free Radical Biology and Medicine*. 2008;44(5):882-892
47. R. M. Lebovitz, H. Zhang, H. Vogel et al., Neurodegeneration, myocardial injury, and perinatal death in mitochondrial superoxide dismutase-deficient mice. *Proceedings of the National Academy of Sciences of the United States of America*. 1996;93(18):9782-9787.
48. D. C. Wallace. A mitochondrial paradigm of metabolic and degenerative diseases, aging, and cancer: a dawn for evolutionary medicine. *Annual Review of Genetics*. 2005;39:359-407.
49. Hochstrasser T, Marksteiner J, Humpel C. Telomere length is age-dependent and reduced in monocytes of Alzheimer patients. *Exp Gerontol*. 2012 ;47(2):160-3.
50. Von Zglinicki T, Martin-Ruiz CM. Telomeres as biomarkers for ageing and age-related diseases. *Curr Mol Med*. 2005;5(2):197-203.
51. Freund A, Orjalo AV, Desprez PY, Campisi J. Inflammatory networks during cellular senescence: causes and consequences. *Trends Mol Med*. 2010;16(5):238-46.

52. Bartek J, Hodny Z, Lukas J. Cytokine loops driving senescence. *Nat Cell Biol.* 2008;10(8):887-9.
53. Chen QM, Prowse KR, Tu VC, Purdom S, Linskens MH. Uncoupling the senescent phenotype from telomere shortening in hydrogen peroxide-treated fibroblasts. *Exp Cell Res.* 2001;265(2):294-303.
54. Michaloglou C, Vredeveld LC, Soengas MS, Denoyelle C, Kuilman T, van der Horst CM, Majoor DM, Shay JW, Mooi WJ, Peeper DS. BRAFE600-associated senescence-like cell cycle arrest of human naevi. *Nature.* 2005;436(7051):720-4.
55. Lowe SW, Cepero E, Evan G. Intrinsic tumour suppression. *Nature.* 2004;432(7015):307-15.
56. Serrano M, Lin AW, McCurrach ME, Beach D, Lowe SW. Oncogenic ras provokes premature cell senescence associated with accumulation of p53 and p16INK4a. *Cell.* 1997;88(5):593-602.
57. Stein GH, Beeson M, Gordon L. Failure to phosphorylate the retinoblastoma gene product in senescent human fibroblasts. *Science.* 1990;249(4969):666-9.
58. Wei W, Hemmer RM, Sedivy JM. Role of p14(ARF) in replicative and induced senescence of human fibroblasts. *Mol Cell Biol.* 2001;21(20):6748-57.
59. Argraves KM, Wilkerson BA, Argraves WS. Sphingosine-1-phosphate signaling in vasculogenesis and angiogenesis. *World J Biol Chem* 2010;1:291-297.

60. Yusuf A, Hannun & Lina M. Obeid. Principles of bioactive lipid signalling: lessons from sphingolipids. *ature Reviews Molecular Cell Biology* 2008;9:139-150
61. Li MH, Sanchez T, Pappalardo A, Lynch KR, Hla T, Ferrer F. Induction of antiproliferative connective tissue growth factor expression in Wilms' tumor cells by sphingosine-1-phosphate receptor 2. *Mol Cancer Res.* 2008;6(10):1649-56.
62. Stiban J, Tidhar R, Futerman AH. Ceramide synthases: roles in cell physiology and signaling. *Adv Exp Med Biol.* 2010;688:60-71.
63. Pettus BJ, Chalfant CE, Hannun YA. Ceramide in apoptosis: an overview and current perspectives. *Biochim Biophys Acta.* 2002;1585(2-3):114-25.
64. Cuvillier O. Sphingosine in apoptosis signaling. *Biochim Biophys Acta.* 2002 Dec;1585(2-3):153-62.
65. Spiegel S, Kolesnick R. Sphingosine 1-phosphate as a therapeutic agent. *Leukemia.* 2002;16(9):1596-602.
66. Lavieu G, Scarlatti F, Sala G, Carpentier S, Levade T, Ghidoni R, Botti J, Codogno P. Regulation of autophagy by sphingosine kinase 1 and its role in cell survival during nutrient starvation. *J Biol Chem.* 2006;281:8518–8527
67. Xiong Y, Lee HJ, Mariko B, Lu YC, Dannenberg AJ, Haka AS, Maxfield FR, Camerer E, Proia RL, Hla T. Sphingosine kinases are not required for inflammatory responses in macrophages. *J Biol Chem.* 2013;288(45):32563-73.

68. Villena J, Henriquez M, Torres V, Moraga F, Díaz-Elizondo J, Arredondo C, Chiong M, Olea-Azar C, Stutzin A, Lavandero S, Quest AF. Ceramide-induced formation of ROS and ATP depletion triggers necrosis in lymphoid cells. *Free Radic Biol Med.* 2008;44(6):1146-60.
69. Dieter A. Kubli and Åsa B. Gustafsson. Mitochondria and Mitophagy: The Yin and Yang of Cell Death Control. *Circ Res.* 2012; 111(9): 1208–1221.
70. Lisa A. Brennan, Ph.D., Research Assistant Professor and Marc Kantorow, Ph.D., Professor. Mitochondrial function and redox control in the aging eye: Role of MsrA and other repair systems in cataract and macular degenerations. *Exp Eye Res.* 2009; 88(2): 195–203.
71. Shay JW, Pereira-Smith OM, Wright WE. A role for both RB and p53 in the regulation of human cellular senescence. *Exp Cell Res.* 1991;196(1):33-9.
72. Aksoy O, Chicas A, Zeng T, Zhao Z, McCurrach M, Wang X, Lowe SW. The atypical E2F family member E2F7 couples the p53 and RB pathways during cellular senescence. *Genes Dev.* 2012;26(14):1546-57.
73. Heidi M. Sankala, Nitai C. Hait, Steven W. Paugh, et al. Involvement of Sphingosine Kinase 2 in p53-Independent Induction of p21 by the Chemotherapeutic Drug Doxorubicin. *Cancer Res* 2007;67:10466-10474.
74. Douglas C. Wallace. Mitochondria and cancer. *Nat Rev Cancer.* 2012 Oct;12(10):685-98.

75. Kim & Sieburth, Sphingosine Kinase Activates the Mitochondrial Unfolded Protein Response and Is Targeted to Mitochondria by Stress. 2018, Cell Reports 24, 2932–2945.
76. Li, Y., Li, S., Qin, X. et al. The pleiotropic roles of sphingolipid signaling in autophagy. Cell Death Dis 5, e1245 (2014).
77. Megan M. Young, Hong-Gang Wang. Sphingolipids as Regulators of Autophagy and Endocytic Trafficking. Adv Cancer Res. Volume 140, 2018, Pages 27-60.
78. Min Kyung Kim et al. Links between accelerated replicative cellular senescence and down-regulation of SPHK1 transcription. BMB Rep. 2019 Mar;52(3):220-225.
79. Gráinne S. Gorman et al. Mitochondrial diseases. Nature Reviews Disease Primers volume 2, Article number: 16080 (2016).
80. Viktor I.Korolchuk et al. EBioMedicine. Volume 21, July 2017, Pages 7-13.
81. Gerben van Hameren et al. In vivo real-time dynamics of ATP and ROS production in axonal mitochondria show decoupling in mouse models of peripheral neuropathies. Acta Neuropathologica Communications volume 7, Article number: 86 (2019)
82. Brittany A Law et al. Lipotoxic very-long-chain ceramides cause mitochondrial dysfunction, oxidative stress, and cell death in cardiomyocytes. FASEB J. 2018 Mar;32(3):1403-1416.

83. E. Deas, N.W. Wood, H. Plun-Favreau. Mitophagy and Parkinson's disease: the PINK1-parkin link. *Biochim. Biophys. Acta*, 1813 (2011), pp. 623-633.
84. Megan M. Young et al., Sphingosine Kinase 1 Cooperates with Autophagy to Maintain Endocytic Membrane Trafficking. *Cell Reports*, 17(6), 1532-1545.
85. Malene Hansen, David C. Rubinsztein, David W. Walker. Autophagy as a promoter of longevity: insights from model organisms. *Nature Reviews Molecular Cell Biology* volume 19, pages579–593(2018)

국문 요약

지방 유래 중간엽 줄기세포는 자가 증식율을 가진 미분화된 세포로써 분화된 지방 조직에서 쉽게 분리할 수 있으며 분리된 세포는 지방, 연골, 뼈, 신경세포 등으로 재분화 가능하다. 이러한 특성 때문에 다양한 질병의 치료제로써 각광을 받고 있으며 현재 이러한 세포를 이용한 연구가 활발한 진행 중에 있으나, 중간엽 줄기세포는 배아줄기세포와는 다르게 telomere 의 길이가 짧고 In vitro 배양 조건에서 오는 스트레스에 매우 민감하여 몇 차례 계대 배양 진행 후 비가역적 세포 노화에 이르게 되어 젊은 세포를 대량으로 얻기 힘들다는 단점이 있다. 이러한 세포 노화를 지연시키는 연구를 통해 중간엽 줄기세포를 이용한 연구의 단점을 극복한다면 다양한 질병의 세포 치료제를 만드는데 도움이 될 것이다.

본 연구에서는 지방 유래 중간엽 줄기세포의 노화 현상에서 Sphingolipids 의 신진대사를 조절하는 효소인 Sphingosine kinase 1 (SPHK1) 이 중요한 역할을 한다는 것을 확인하였다. 계대 배양 과정에서 세포의 노화가 진행됨에 따라 SPHK1 의 발현이 감소하는 것을 확인하였고, 어린 지방 유래 중간엽 줄기세포에 shRNA 를 이용하여 SPHK1 의 발현을 억제하였을 때 BrdU uptake 를 통해 세포 증식률이 감소되는 것과 노화 단백질 표지자인 P-p53 (S15), p21, P-pRb 의 변화 및 SA-β-gal 염색을 통해 비가역적 세포 노화가 일어나는 것을 확인하였다. 또한 노화된 지방 유래 중간엽 줄기세포에서 Sphingolipids 대사 변화를 확인한 결과 Sphingosine, Sphinganine,

16:0 Ceramide, 16:0 Sphingomyelin 의 양이 매우 증가해 있다는 것을 확인하였고, 이 같은 결과는 SPHK1 의 발현이 감소된 상황에서도 동일한 양상을 보임을 확인하였다. 이 결과들을 통해 SPHK1 억제에 의해 유도되는 세포 노화 현상에 anti-growth 요소로 잘 알려진 Ceramide 의 양적 변화가 영향을 미치는지 확인하게 위해 SPHK1 의 발현이 억제된 세포에 Ceramide 합성을 억제하는 약물인 Fumonisine B1 을 처리한 결과 증가된 세포 노화 현상이 회복되지 못하였다. 하여 SPHK1 감소로 인해 pro-growth 요소인 Sphingosine 1-phosphate (S1P) 가 생성되지 못하여 세포 노화 현상이 유도된다 가정하고 SPHK1 이 억제된 세포에 S1P 처리하였지만 이 역시 세포 노화 현상을 회복시키지 못하였다. 이에 SPHK1 의 발현 감소로 인해 세포 노화 현상이 유도된 세포에 Fumonisine B1 과 S1P 를 모두 처리하여 증가된 Ceramide 의 양을 억제하고 감소된 S1P 를 보충하니 SA-β-gal 염색을 통해 세포 노화 현상이 회복됨을 확인하였다. 최근 연구들 중 ceramide 와 S1P 가 미토콘드리아 기능 장애와 연관성이 보고된 바 있어 이를 확인하고자 shRNA 를 통해 SPHK1 의 발현을 억제시킨 후 미토콘드리아 기능을 확인하였다. 그 결과 oxygen consumption rate, NAD⁺/NADH ratio 증가 되었으나 reactive oxygen species 와 proton leak 이 함께 증가되어 미토콘드리아 uncoupling 이 일어났으며 기능 장애 미토콘드리아가 증가하여 glycolysis 쪽으로 에너지 대사가 기울어져 있음을 확인하였다. 또한 SPHK1 의 발현이 억제된 세포에서는 이러한 기능장애 미토콘드리아 제거를 위한 대표적인 메커니즘인 마이토파지가 잘 진행되지 않음을 LC3B 발현을 통해 확인하였으며, 단계적 오토파지 메커니즘을 확인한 결과 ATG5-12 conjugated form 이 감소되어 초기 nucleation 과정이 억제됨을 확인하였고

이를 통해 기능 장애 미토콘드리아가 축적된다는 결론에 이르렀다. 이 모든 결과들을 토대로 SPHK1 이 억제되었을 때 일어나는 Ceramide 의 양적 증가 및 SIP 의 양적 감소가 미토콘드리아 기능장애를 유발하고 지방 유래 중간엽 줄기세포의 노화 현상에 영향을 미치는 것을 확인하였으며, 이 결과를 바탕으로 지방 유래 중간엽 줄기세포를 이용한 세포 치료제 개발의 한계를 해결할 수 있는 중요한 기초 자료를 제공할 것이라 기대한다.

중심 단어: 지방 유래 중간엽 줄기세포, 세포 노화 현상, SPHK1, Ceramide, SIP, 미토콘드리아, 오토파지